INFECTION AND IMMUNITY, June 2003, p. 3572–3577 Vol. 71, No. 6
0019-9567/03/$08.00+0 DOI: 10.1128/IAI.71.6.3572–3577.2003

Helicobacter-Induced Chronic Active Lymphoid Aggregates Have Characteristics of Tertiary Lymphoid Tissue

Nirah H. Shomer,[1]†* James G. Fox,[2] Amy E. Juedes,[3]‡ and Nancy H. Ruddle[3]

Section of Comparative Medicine, Yale University, New Haven, Connecticut 06510[1]; Massachusetts Institute of Technology, Division of Comparative Medicine, Cambridge, Massachusetts 02139[2]; and Department of Epidemiology and Public Health and Section of Immunobiology, Yale University School of Medicine, New Haven, Connecticut 06520-8034[3]

Received 10 December 2002/Returned for modification 10 February 2003/Accepted 19 March 2003

Susceptible strains of mice that are naturally or experimentally infected with murine intestinal helicobacter species develop hepatic inflammatory lesions that have previously been described as chronic active hepatitis. The inflammatory infiltrates in some models of chronic autoimmunity or inflammation resemble tertiary lymphoid organs hypothesized to arise by a process termed lymphoid organ neogenesis. To determine whether hepatic inflammation caused by infection with helicobacter could give rise to tertiary lymphoid organs, we used fluorescence-activated cell sorting, immunohistochemistry, and in situ hybridization techniques to identify specific components characteristic of lymphoid organs in liver tissue sections and liver cell suspensions from helicobacter-infected mice. Small venules (high endothelial venules [HEVs]) in inflammatory lesions in *Helicobacter* species-infected livers were positive for peripheral node addressin. Mucosal addressin cell adhesion molecule also stained HEVs and cells with a staining pattern consistent with scattered stromal cells. The chemokines SLC (CCL 21) and BLC (CXCL13) were present, as were B220-positive B cells and T cells. The latter included a naïve (CD45lo-CD62Lhi) population. These findings suggest that helicobacter-induced chronic active hepatitis arises through the process of lymphoid organ neogenesis.

Tertiary lymphoid tissue is a term describing ectopic lymphoid aggregates that accumulate during the process of chronic immune stimulation. Tertiary lymphoid organs exhibit characteristics usually associated with the secondary lymphoid organs (lymph nodes, Peyer's patches, and the spleen). These characteristics include cellular composition, endothelial venule-like vessels with expression of adhesion molecules, and expression of constitutive or lymphoid organ chemokines. Morphological features of lymphoid organs include compartmentalization of B-cell and T-cell populations and the presence of high endothelial venules (HEV) that are the site of lymphocyte extravasation into the lymph node parenchyma. HEVs are identified morphologically or by the expression of peripheral node addressin (PNAd) or mucosal addressin cell adhesion molecule (MAdCAM). B-lymphocyte-attracting chemokine CXCL 13 (BLC) and T-lymphocyte-attracting secondary lymphocyte-attracting chemokine CCL 21 (SLC) are constitutively expressed in secondary lymphoid organs and have also been found in tertiary lymphoid tissue (11). These chemokines are crucial for lymphoid organ development. Ectopic expression of BLC in the pancreas of transgenic mice leads to lymphotoxin (LT)-dependent development of lymph node-like structures that contain compartmentalized B and T cell areas, HEVs, and SLC (16). Tertiary lymphoid organs have been described in the chronic organ-specific inflammation in several autoimmune diseases. These include the thyroiditis with prominent germinal centers in Hashimoto's disease (13), the synovitis with plasma cells and isotype switching in the joints in rheumatoid arthritis (1), and the insulitis in the nonobese diabetic mouse with expression of endothelial addressins PNAd and MAdCAM (6) and BLC (11). The term lymphoid organ neogenesis (20) has been proposed to define the process by which this occurs, based in part on the development of such tertiary lymphoid organs in the pancreas of a mouse transgenic for the rat insulin promoter-driving expression of LT-α (14). The fact that LT plays a crucial role in the development of secondary lymphoid organs, in that LT-$\alpha^{-/-}$ mice are devoid of lymph node and Peyer's patches and exhibit defects in splenic organization (4), provides a unifying model for this concept.

Recently it has become apparent that chronic inflammation associated with a few infectious diseases also exhibits some characteristics of tertiary lymphoid organs. These diseases include Lyme arthritis (23), hepatitis C-induced liver inflammation (9), and *Propriobacterium acnes* infection of mouse liver (27). *Helicobacter pylori* infection in humans can give rise to accumulations of lymphoid cells in the gastric mucosa with the expression of MAdCAM and PNAd (5). More recently, BLC has been noted in the *H. pylori*-infected gastric mucosa (17). In some cases, lymphomas also develop in the course of this infection, and they also retain some characteristics of lymphoid organs with PNAd, SLC, and accumulation of L-selectin (naïve) T cells. Experimental infection of mice (15) and guinea pigs (22) with *H. pylori* stimulates the appearance of gastric lymphoid follicles with prominent germinal centers. Chronic infection of mice with *Helicobacter hepaticus* (25) stimulates the development of large hepatic inflammatory infiltrates that

* Corresponding author. Mailing address: Laboratory Animal Science Center, 715 Albany St., W707, Boston, MA 02118. Phone: (617) 638-4090. Fax: (617) 638-4055. E-mail: nirah@bu.edu.

† Present address: Boston University, Laboratory Animal Science Center, Boston, MA 02118.

‡ Present address: LaJolla Institute of Allergy and Immunology, San Diego, CA 92121.

have some morphological similarities to tertiary lymphoid tissue. A novel urease-negative *Helicobacter* sp. that leads to similar hepatic inflammation was recently described (21).

In this study, we have investigated the possibility that helicobacter infection in mice gives rise to accumulations of lymphoid cells with the characteristics of lymphoid organs. Infection with the novel *Helicobacter* sp. produces severe cholangiohepatitis after inoculation into susceptible strains of mice. We applied the same criteria of tertiary lymphoid organs that have been previously applied to autoimmune diseases and transgenic mice. Our observation that helicobacter infection in the mouse gives rise to tertiary lymphoid organs as defined by cellular composition, endothelial addressins, and lymphoid organ chemokines provides a new model to study the mechanism of this process. These data also suggest that lymphoid organ neogenesis is a process that is applicable in chronic inflammation in both autoimmune and infectious diseases and could play a role in pathogenesis and/or protection.

MATERIALS AND METHODS

Animals. Five-week-old male A/J mice (Jackson Laboratories, Bar Harbor, Maine) were maintained in a facility accredited by the Association for the Assessment and Accreditation of Laboratory Animal Care, International. Animals were free of rodent viral, parasitic, and bacterial pathogens, including all *Helicobacter* species. Animals were maintained at a constant temperature of 70 to 72°C and 40 to 70% humidity, with 10 to 15 air changes per hour. All manipulations performed on the mice were approved by the Institutional Animal Care and Use Committee.

Bacteria. The novel urease-negative *Helicobacter* sp. was grown from a stock originally isolated from the cecum of a clinically normal feral mouse (MIT 96-1001). It was grown under microaerobic conditions in vented jars containing N_2, H_2, and CO_2 (80:10:10) at 37°C in brucella broth supplemented with 5% fetal calf serum. The bacteria were harvested after 24 to 48 h of growth, resuspended in phosphate-buffered saline (PBS), and visualized by Gram stain and phase microscopy for purity, morphology, and motility. The optical density at 600 nm was adjusted to 1.0, and 0.3 ml of this inoculum (corresponding to approximately 3×10^7 CFU) was used for each intraperitoneal injection or oral dose.

Infection status. To confirm infection status, cecal contents or liver collected at necropsy were cultured as previously described (21). Cecal contents were applied directly to blood agar plates containing cefoperazone, vancomycin, and amphotericin B (Remel, Lenexa, Kans.). Aseptically collected liver was ground and applied directly to blood agar plates for isolation of the *Helicobacter* sp. Although growth of the *Helicobacter* sp. was generally evident within 5 days, plates were maintained for 2 weeks before a determination of no growth was made. Presence of the *Helicobacter* sp. was determined by characteristic colony morphology, bacterial morphology, and urease and catalase tests. Selected cecal samples were analyzed by PCR to confirm positive or negative status. Samples were analyzed using helicobacter genus-specific primers as previously described (21).

Tissue sections for immunohistochemistry and in situ analysis. Liver tissue was obtained from mice that were confirmed to be infected or uninfected (controls) with the *Helicobacter* sp. Mice were euthanized for tissue harvest at 7 weeks ($n = 20$ controls and 20 infected), 14 weeks ($n = 10$ controls and 10 infected), or 24 weeks ($n = 17$ controls and 17 infected) postinfection. (Not all mice were used for all types of evaluation; see Results for details.) For immunohistochemistry, livers were embedded in Tissue-Tek OCT compound (VWR Scientific, Bridgeport, N.J.) and frozen or were fixed in formalin or Carnoy's fixative and embedded in paraffin. For in situ hybridization, livers were fixed overnight in 4% paraformaldehyde in PBS, then fixed for an additional 48 h in 4% paraformaldehyde–30% sucrose in PBS and then snap-frozen in Tissue-Tek OCT compound (VWR Scientific) and stored at −70°C. Slides made from frozen blocks were used for immunohistochemistry without further processing. Paraffin-embedded slides were de-paraffinized in 100% xylene (three 3-min washes followed by three 3-min washes in 100% ethanol). Carnoy's-fixed tissues were used immediately after deparaffinization. For formalin-fixed tissues, antigen recovery was aided by incubating slides for 30 min in a solution of Tris-buffered saline with 4 mM $CaCl_2$ and 0.25% trypsin.

Cell suspensions for FACS. Infected ($n = 3$) or control ($n = 3$) A/J mice at 24 weeks postinfection were euthanized by CO_2 asphyxiation, and their livers were perfused via the portal vein, as described by Mehal et al. (19), with RPMI 1640 medium (Life Technologies, Gaithersburg, Md.) containing collagenase II (Sigma, St. Louis, Mo.) at 1 mg/ml. The livers were then ground; the resulting cell suspensions were incubated at 37°C for 2 h, and mononuclear cells were isolated by discontinuous Percoll (PharMacia, Piscataway, N.Y.) gradient. After blocking with purified rat, hamster, and goat immunoglobulin G (Pierce, Rockford, Ill.), cells were incubated with directly conjugated antibodies in fluorescence-activated cell sorter (FACS) buffer (1% bovine serum albumin–0.1% sodium azide in PBS). Samples were analyzed with a FACScan flow cytometer (Becton Dickinson) with Cellquest software.

Immunohistochemical staining. Tissues were first blocked for 30 min with 3% serum of the species in which the secondary antibody was made, then incubated for 1 h with the primary antibody and then incubated for 30 min with the biotinylated secondary antibody at a dilution of 1:250. They were visualized with strepavidin-conjugated alkaline phosphatase (ABC kit; Vector Labs, Burlingame, Calif.) and the Vector Red kit (Vector Labs) or with strepavidin-conjugated horseradish peroxidase (ABC Elite; Vector Labs) and VIP kit (Vector Labs). Buffer was 100 mM Tris HCl (pH 8.2)–0.01% Triton X–1% bovine serum albumin (Sigma) for the alkaline phosphatase kits. PBS (pH 7.5) was used instead of Tris HCl for the ABC Elite kit. A nonspecific antibody of the same isotype as the primary antibody was used as a negative control.

Antibodies. (i) FACS. The CD4-fluorescein isothiocyanate (FITC), B220-phycoerythrin (PE), immunoglobulin M-FITC, CD69-PE, Mac-1-PE, L-selectin-PE, and CD44-Cychrome CD4-FITC, CD11b (Mac-1)-FITC, CD45-Cy-Chrome antibodies were all from Pharmingen (San Diego, Calif.).

(ii) Immunohistochemistry. Primary antibodies (all obtained from Pharmingen) were monoclonal antibodies that react with MAdCAM-1 (MECA 367), PNAd (MECA 79), VCAM-1, B220, and CD3. MECA 79 was used at a concentration of 5 μg/ml; 3% mouse serum (Sigma) was used for blocking, the secondary antibody was biotinylated immunoglobulin-κ light chains (Pharmingen), and unlabeled immunoglobulin-κ light chains (Pharmingen) were used as a negative control. MECA 367 was used at a concentration of 5 μg/ml. Three percent goat serum (Sigma) was used to block, the secondary antibody was biotinylated goat anti-rat immunoglobulin G (Pharmingen), and the negative control was unlabeled Rat immunoglobulin G2a (Pharmingen). Anti-B220 and anti-VCAM-1 were used at a concentration of 2 μg/ml, and the block, secondary, and control antibodies used were identical to those for MECA 367. CD3 was used at a concentration of 2 μg/ml; the secondary antibody was biotinylated anti-hamster.

In situ hybridization. Digoxigenin (DIG)-labeled BLC and SLC antisense and sense probes were prepared by in vitro transcription from I.M.A.G.E. consortium expressed sequence tags 596050 and 389013, obtained from Genome Systems (St. Louis, Mo.), as previously described (11). Transcript yield and integrity of the probes were determined by comparison with control DIG-labeled RNA (Boehringer Mannheim, Mannheim, Germany). In situ hybridization was done as previously described with fixed frozen tissue sections of 5- to 10-μm thickness cut onto poly-L-lysine-treated glass slides (11). In brief, sections were fixed in 4% paraformaldehyde, pretreated with proteinase K (Boehringer Mannheim) and acetic anhydride, prehybridized, hybridized overnight at 58°C with the DIG-labeled riboprobes, washed at high stringency, incubated with anti-DIG antibody conjugated to alkaline phosphatase (Boehringer Mannheim), and developed with nitro blue tetrazolium/5-bromo-4-chloro-3-indole-phosphate.

RESULTS

Infection with a novel urease-negative *Helicobacter* sp. results in hepatic lesions. Livers from uninfected control mice had no lesions. Livers from experimentally infected mice at 7, 14, or 24 weeks postinfection had accumulations of mononuclear cells surrounding portal areas, with dense accumulations of cells surrounding the bile ducts (peribiliary inflammation) and inflammatory cells seen inside ducts and migrating through bile duct walls (cholangiohepatitis). In addition, significant infiltrates surrounded portal blood vessels. Morphologically, by hematoxylin and eosin staining, there were lymphocytes, macrophages, and plasma cells, with rare neutrophils (Fig. 1A). To determine if these aggregates represented tertiary lymphoid tissue, we performed qualitative and quantita-

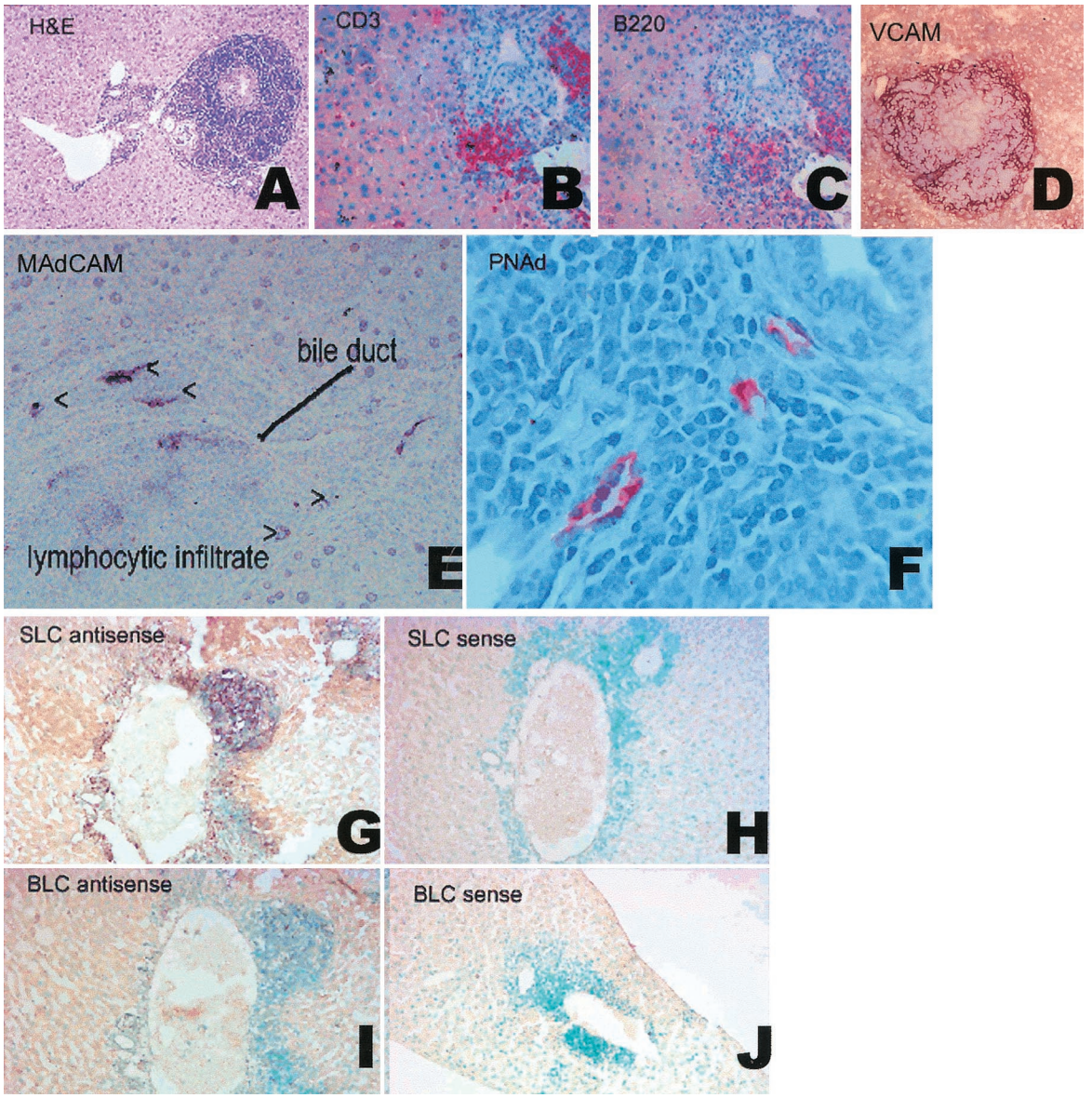

FIG. 1. Formation of lymphoid tissue in *Helicobacter* sp.-infected mouse livers. (A) Hematoxylin and eosin photomicrograph of a typical inflammatory infiltrate at 24 weeks postinfection. (B-C) Serial sections of mouse liver (7 weeks postinfection) stained for CD3-positive T cells (B) and B220-positive B cells (C). Clusters of $CD3^+$ T cells are present, and B220 staining shows B-cell clusters colocalizing with, but separate from, T-cell clusters. (D) VCAM: dark red diffuse staining is visible in areas of intense inflammatory infiltrate (7 weeks postinfection). (E-F) Blood vessels develop a morphology resembling HEV and express MAdCAM-1 (E) and PNAd (F) (7 weeks postinfection). (G-H) In situ hybridization analysis of SLC mRNA expression mouse livers using DIG-labeled RNA probes. (G) Expression of SLC is indicated by purple staining of cells with SLC-antisense probes. (H) No staining is seen with SLC sense probe. Infiltrating cells are counterstained with methyl green. (I-J) In situ hybridization analysis of BLC mRNA expression mouse livers using DIG-labeled RNA probes. (I) Expression of BLC is indicated by purple staining of cells with BLC-antisense probes. (J) No staining is seen with BLC sense probe. Infiltrating cells are counterstained with methyl green.

tive analyses of the cell types, addressins, and chemokines present in the infiltrates.

The cellular populations in *Helicobacter* sp. liver infiltrates included cell types associated with lymphoid organs. The presence and phenotype of infiltrating cells' populations were determined by immunohistochemistry and FACS. Liver sections were stained with monoclonal antibodies against B220 and CD3 (markers of B and T cells, respectively). No staining was seen in livers from control mice ($n = 7$). In mice infected for 24 weeks ($n = 7$), approximately one-third of the cells in the inflammatory infiltrate were positive for CD3 (Fig. 1B), one-third were B220 positive B cells (Fig. 1C), and some cells appeared to stain with neither antibody. In serial sections (Fig. 1A and B), it was apparent that B and T cells were present in separate aggregates and thus exhibited the compartmentalization characteristic of lymphoid organs. FACS was used to phenotype and quantitate cell types in livers from infected ($n = 3$) and uninfected ($n = 3$) mice at 24 weeks postinfection. Approximately 10 times more cells were recovered from the livers (6×10^6 to 16×10^6 per liver) of infected mice than from

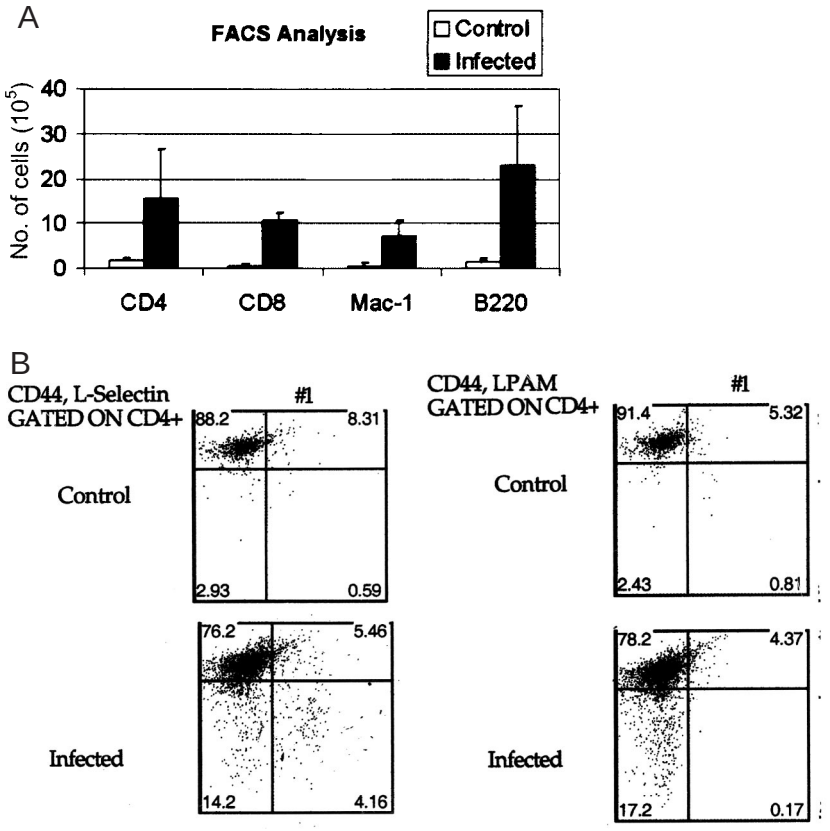

FIG. 2. FACS analysis of mononuclear cells from liver infiltrates (results shown are the means of results of three experiments). (A) Cells isolated from infected and uninfected mice at 24 weeks postinoculation were labeled with Mac-1, CD4, CD8, and B220. Infected livers had quantitatively more cells than livers from uninfected controls. (B) Cells were gated for naïve T cells (low CD44 expression), and numbers of LPAM- or CD62L-positive cells are shown in the bottom right quadrant of each panel. L-selectin-positive cells, but not LPAM-positive cells, were actively recruited to the livers of infected mice.

age-matched uninfected sham-dosed controls (Fig. 2A). Cells isolated included $CD4^+$, $CD8^+$, B220+, and Mac-1+ cells. The proportions were approximately 1:1 for T cells to B cells and approximately 1:1 for CD4 to CD8 cells in both infected and uninfected mice. Mac-1+ cells were approximately 10% of the population of total cells. A small percentage were CD11c+, a characteristic of dendritic cells. The T-cell population included both L-selectin^{hi}CD44lo and L-selectin^{lo} CD44^{hi} populations, respectively, characteristic of naïve and memory T cells. A very small population of the CD44^{lo} cells were LPAM+ ($\alpha4\beta7$). Results are summarized in Fig. 2B. These data indicate that the hepatic inflammation in *Helicobacter* sp.-infected livers exhibits characteristics of lymphoid organs, namely cellular population (B, T, and antigen-presenting cells), compartmentalization into T and B cell areas, and the presence (though in low numbers) of cells with a naïve phenotype.

***Helicobacter* sp. liver infiltrates exhibited adhesion molecules and addressins characteristic of lymphoid organs.** To determine if blood vessels in the inflammatory infiltrates included those with characteristics of HEVs, which are identified by the presence of specific addressins, liver sections were stained with monoclonal antibodies for the addressins MAdCAM and PNAd (Fig. 1E and F). In addition, selected sections were stained with VCAM (a marker of inflammation) (Fig. 1D). Some vessels in the infiltrates stained strongly and specifically for PNAd (Fig. 1F). MECA 367 (anti-MAdCAM) also labeled HEVs in areas of intense inflammation and in addition labeled scattered cells in a pattern consistent with dendritic cells (Fig. 1E). Both PNAd and MAdCAM staining were seen only in areas of intense inflammation and dense peribiliary infiltrates. PNAd staining was also seen rarely in structures morphologically identified as bile ducts (not shown). No staining was seen in uninflamed areas of the liver or in liver sections from uninfected control mice. PNAd was identified in liver sections from 20 of 20 mice infected for 7 weeks, 10 of 10 mice infected for 14 weeks, and 17 of 17 mice infected for 24 weeks. MAdCAM was identified in only about half of sections examined at early time points (5 of 10 at 7 weeks, 7 of 10 at 14 weeks, and 6 of 7 at 24 weeks) and only in areas of extensive inflammation (which tended to occur predominantly at the later time points). Blood vessel endothelia did not stain with VCAM; however, VCAM staining was observed in a diffuse pattern associated with intense inflammatory infiltrates but not with HEVs (Fig. 1D). HEVs are specialized vessels found specifically in lymphoid organs. Identification of HEV-specific addressins in these inflammatory infiltrates strongly supports

the notion that the infiltrates exhibit characteristics of lymphoid organs.

***Helicobacter* sp. liver infiltrates expressed chemokines characteristic of lymphoid organs.** SLC and BLC are chemokines usually considered to be characteristic of secondary lymphoid organs, such as spleen or lymph nodes. SLC is capable of attracting dendritic cells and T cells, and BLC attracts B cells. In order to determine whether these chemokines characteristic of lymphoid organs were expressed in *Helicobacter* sp.-induced inflammatory lesions, selected fixed frozen liver sections were evaluated by in situ hybridization with anti-sense probes for SLC (Fig. 1G and H) and BLC (Fig. 1I and J). Both chemokine mRNAs were detected in regions of intense inflammatory infiltration but were not present in noninflamed areas of infected livers at 7 or 24 weeks postinfection ($n = 3$ at each time point) or in uninfected livers ($n = 3$ at each time point). The chemokines colocalized with B- and T-cell infiltrates. Thus, one more characteristic of lymphoid organs is present in the *Helicobacter* sp.-induced infiltrates.

DISCUSSION

The purpose of this study was to determine whether the inflammatory infiltrates in *Helicobacter* sp. cholangiohepatitis include characteristics of tertiary lymphoid tissue. Evidence supporting this hypothesis includes the finding that the hepatic inflammatory infiltrates contained appropriate cellular populations, addressins, and chemokines. Compartmentalization of B and T cell populations was also evident, although germinal centers, such as those present in the gastric lymphoid follicles caused by *H. pylori* infection, were not apparent morphologically in these mice. Additional criteria not addressed in this study include certain morphological features, such as lymphatics and the presence of active antigen presentation. Only indirect evidence for antigen presentation (the presence of Mac1+ and CD11c+ cells) was obtained. SLC is an important chemoattractant for dendritic cells both in vivo and in vitro. Dendritic cells were present in the livers of infected mice, and it will be interesting to see if these cells have been recruited by SLC by studying mice deficient in this ligand or its receptor.

The inflammatory infiltrates expressed both MAdCAM and PNAd, which are endothelial cell addressins involved in the trafficking of naïve LPAM+ and L-selectin+ T cells into Peyer's patches and lymph nodes, respectively. PNAd was expressed in both the vessels and bile ducts in inflamed portal tracts. PNAd expression has not previously been reported to be expressed in any tissues other than HEVs, so finding it in inflamed bile ducts was not expected. However, in primary biliary cirrhosis, damaged bile ducts have been shown to express ICAM and in some cases VCAM (26). These authors suggest that the presence of these adhesion molecules facilitates recruitment of inflammatory cells to the bile ducts in primary biliary cirrhosis. Both MAdCAM and PNAd staining were detected in liver tissues from mice 7, 14, and 24 weeks postinfection with helicobacter. At 24 weeks postinfection (the only time point at which livers were available for FACS analysis), L-selectin-positive, but not LPAM-positive, T cells were present in numbers higher than in control mice, suggesting that the PNAd, but not MAdCAM, was actively recruiting relevant (L-selectin-positive) cells at this time point. It is possible that at earlier time points, MAdCAM was more important in recruitment but that at the later time point, much of the MAdCAM had been replaced by PNAd, as occurs in the development of secondary lymphoid organs (18). Future studies will evaluate the kinetics of addressin expression. VCAM was also detected, confirming that classical inflammation was also present. VCAM stained the endothelium of very few vessels but did exhibit a diffuse staining pattern in areas of lymphoid aggregates. This pattern is consistent with the VCAM staining pattern reported in stomach biopsies of patients infected with *H. pylori* (7).

The presence of B cells, T cells, and dendritic cells all could be due to recruitment by chemokines. We concentrated on lymphoid chemokines here, but it is likely that inflammatory chemokines are also expressed. The importance here is that SLC and BLC, which are lymphoid-specific chemokines, are expressed in *Helicobacter* infection, confirming that infection with these organisms can give rise to tissue with characteristics of tertiary lymphoid organs.

There are several possible mechanisms by which *Helicobacter* species could induce tertiary lymphoid tissue. *Helicobacter* may induce the formation of lymphoid tissue by causing inflammation and damage, by inducing lymphoid organ-promoting or chemokines directly, or even by mimicking the signals for lymphoid organogenesis. One fascinating possibility is that *Helicobacter* may express or direct the formation of an L-selectin ligand. The MECA79 (PNAd) epitope derives from modifications of a variety of core protein precursors, including CD34, GlyCAM, podocalyxin, and MAdCAM. *H. pylori* expresses a Lewis X analogue via a bacterial fucosyl transferase (24). Lewis X becomes an L-selectin ligand when modified by a GlcNac6 sulfotransferase (3). It is possible that cellular or bacterial proteins modify a *Helicobacter* Lewis X analogue to generate the MECA 79 epitope. One candidate sulfotransferase, HECGlcNAC6ST, is expressed primarily in HEVs (2, 10) and has been shown to be crucial for the luminal expression of the high-affinity L-selectin ligand MECA 79 epitope (8). An intriguing possibility is that HECGlcNAC6ST is activated in the context of *Helicobacter* species infection and induces the expression of an L-selectin ligand on *Helicobacter* so that the *Helicobacter* organisms themselves directly attract naïve T cells. MECA 79 detection in the bile ducts of infected mice may represent detection of L-selectin ligand-expressing *Helicobacter* organisms resident in the bile ducts. It is yet to be determined whether the *Helicobacter* sp. studied here in fact expresses a Lewis X analogue and whether that analogue could function as an L-selectin ligand.

In this report, we have presented further evidence that the development of tertiary lymphoid tissue in chronic inflammation involves the same mechanisms as lymphoid organogenesis during development, namely, induction of chemokines and adhesion molecules. Kratz et al. (14) have previously shown that LT is important for local recruitment of both lymphoid and antigen-presenting cells and orchestrates lymphoid neogenesis during the immune response through regulation of adhesion molecules and chemokines normally found in secondary lymphoid organs. It would be extremely interesting to determine whether LT knockout mice are able to form hepatic lymphoid aggregates such as those seen in the A/J mice used in this study. Yoneyama et al. (27) have recently reported on the

presence of adhesion molecules and chemokines in granulomatous inflammatory infiltrate in mice infected with *Propionibacterium acnes*, suggesting that the process of lymphoid neo-organogenesis probably has some universal features independent of host cell type, gram negativity of the organism, or type of inflammation.

Formation of lymphoid follicles occurs in a number of chronic inflammatory diseases, including *H. pylori* gastritis. The function of this tissue is not clear: it may provide functional protection against the agent by allowing antigen presentation at the local site and priming of naïve cells. On the other hand, the tertiary lymphoid tissue may be detrimental to the health of the animal. For example, infection with *H. hepaticus* results in persistent infection, hepatic inflammation, and eventually hepatocellular carcinoma in A/J mice, but in C57BL/6 mice, it results in very little inflammation and no carcinoma (though the C57BL/6 remain persistently infected) (12). A detailed understanding of the processes leading to this lymphoid neogenesis, and determination of what protective role this tertiary lymphoid tissue provides, may provide a rationale for development of new therapeutics that can specifically target this process.

Future studies in the model described here will allow us to determine whether antigen presentation occurs in the liver infiltrate and whether this contributes to protection.

ACKNOWLEDGMENTS

This study was supported by NIH grants NCI CA 16885 (N.H.R.), NIH T32 AI 07019 (A.E.J.), RO1-CA 67529 (J.G.F.), and NIDDKD P30-DK34989-17 (N.H.S.) and by a Richard Gershon Fellowship (A.E.J.).

REFERENCES

1. **Berek, C., and H. J. Kim.** 1997. B-cell activation and development within chronically inflamed synovium in rheumatoid and reactive arthritis. Semin. Immunol. **9:**261–268.
2. **Bistrup, A., S. Bhakta, J. K. Lee, Y. Y. Belov, M. D. Gunn, F. R. Zuo, C. C. Huang, R. Kannagi, S. D. Rosen, and S. Hemmerich.** 1999. Sulfotransferases of two specificities function in the reconstitution of high endothelial cell ligands for L-selectin. J. Cell Biol. **145:**899–910.
3. **Bowman, K. G., B. N. Cook, C. L. de Graffenried, and C. R. Bertozzi.** 2001. Biosynthesis of L-selectin ligands: sulfation of sialyl Lewis x-related oligosaccharides by a family of GlcNAc-6-sulfotransferases. Biochemistry **40:**5382–5391.
4. **De Togni, P., J. Goellner, N. H. Ruddle, P. R. Streeter, A. Fick, S. Mariathasan, S. C. Smith, R. Carlson, L. P. Shornick, J. Strauss-Schoenberger, et al.** 1994. Abnormal development of peripheral lymphoid organs in mice deficient in lymphotoxin. Science **264:**703–707.
5. **Dogan, A., M. Du, A. Koulis, M. J. Briskin, and P. G. Isaacson.** 1997. Expression of lymphocyte homing receptors and vascular addressins in low-grade gastric B-cell lymphomas of mucosa-associated lymphoid tissue. Am. J. Pathol. **151:**1361–1369.
6. **Hanninen, A., C. Taylor, P. R. Streeter, L. S. Stark, J. M. Sarte, J. A. Shizuru, O. Simell, and S. A. Michie.** 1993. Vascular addressins are induced on islet vessels during insulitis in nonobese diabetic mice and are involved in lymphoid cell binding to islet endothelium. J. Clin. Investig. **92:**2509–2515.
7. **Hatz, R. A., G. Rieder, M. Stolte, E. Bayerdorffer, G. Meimarakis, F. W. Schildberg, and G. Enders.** 1997. Pattern of adhesion molecule expression on vascular endothelium in Helicobacter pylori-associated antral gastritis. Gastroenterology **112:**1908–1919.
8. **Hemmerich, S., A. Bistrup, M. S. Singer, A. van Zante, J. K. Lee, D. Tsay, M. Peters, J. L. Carminati, T. J. Brennan, K. Carver-Moore, M. Leviten, M. E. Fuentes, N. H. Ruddle, and S. D. Rosen.** 2001. Sulfation of L-selectin ligands by an HEV-restricted sulfotransferase regulates lymphocyte homing to lymph nodes. Immunity **15:**237–247.
9. **Hillan, K. J., K. E. Hagler, R. N. MacSween, A. M. Ryan, M. E. Renz, H. H. Chiu, R. K. Ferrier, G. L. Bird, A. P. Dhillon, L. D. Ferrell, and S. Fong.** 1999. Expression of the mucosal vascular addressin, MAdCAM-1, in inflammatory liver disease. Liver **19:**509–518.
10. **Hiraoka, N., B. Petryniak, J. Nakayama, S. Tsuboi, M. Suzuki, J. C. Yeh, D. Izawa, T. Tanaka, M. Miyasaka, J. B. Lowe, and M. Fukuda.** 1999. A novel, high endothelial venule-specific sulfotransferase expresses 6-sulfo sialyl Lewis(x), an L-selectin ligand displayed by CD34. Immunity **11:**79–89.
11. **Hjelmstrom, P., J. Fjell, T. Nakagawa, R. Sacca, C. A. Cuff, and N. H. Ruddle.** 2000. Lymphoid tissue homing chemokines are expressed in chronic inflammation. Am. J. Pathol. **156:**1133–1138.
12. **Ihrig, M., M. D. Schrenzel, and J. G. Fox.** 1999. Differential susceptibility to hepatic inflammation and proliferation in AXB recombinant inbred mice chronically infected with Helicobacter hepaticus. Am. J. Pathol. **155:**571–582.
13. **Kasajima, T., M. Yamakawa, and Y. Imai.** 1987. Immunohistochemical study of intrathyroidal lymph follicles. Clin. Immunol. Immunopathol. **43:**117–128.
14. **Kratz, A., A. Campos-Neto, M. S. Hanson, and N. H. Ruddle.** 1996. Chronic inflammation caused by lymphotoxin is lymphoid neogenesis. J. Exp. Med. **183:**1461–1472.
15. **Lee, A., J. G. Fox, G. Otto, and J. Murphy.** 1990. A small animal model of human Helicobacter pylori active chronic gastritis. Gastroenterology **99:**1315–1323.
16. **Luther, S. A., T. Lopez, W. Bai, D. Hanahan, and J. G. Cyster.** 2000. BLC expression in pancreatic islets causes B cell recruitment and lymphotoxin-dependent lymphoid neogenesis. Immunity **12:**471–481.
17. **Mazzucchelli, L., A. Blaser, A. Kappeler, P. Scharli, J. A. Laissue, M. Baggiolini, and M. Uguccioni.** 1999. BCA-1 is highly expressed in Helicobacter pylori-induced mucosa-associated lymphoid tissue and gastric lymphoma. J. Clin. Investig. **104:**R49–R54.
18. **Mebius, R. E., P. R. Streeter, S. Michie, E. C. Butcher, and I. L. Weissman.** 1996. A developmental switch in lymphocyte homing receptor and endothelial vascular addressin expression regulates lymphocyte homing and permits CD4+ CD3- cells to colonize lymph nodes. Proc. Natl. Acad. Sci. USA **93:**11019–11024.
19. **Mehal, W. Z., A. E. Juedes, and I. N. Crispe.** 1999. Selective retention of activated CD8+ T cells by the normal liver. J. Immunol. **163:**3202–3210.
20. **Ruddle, N. H.** 1999. Lymphoid neo-organogenesis: lymphotoxin's role in inflammation and development. Immunol. Res. **19:**119–125.
21. **Shomer, N. H., C. A. Dangler, M. D. Schrenzel, M. T. Whary, S. Xu, Y. Feng, B. J. Paster, F. E. Dewhirst, and J. G. Fox.** 2001. Cholangiohepatitis and inflammatory bowel disease induced by a novel urease-negative Helicobacter species in A/J and Tac:ICR:HascidfRF mice. Exp. Biol. Med. (Maywood) **226:**420–428.
22. **Shomer, N. H., C. A. Dangler, M. T. Whary, and J. G. Fox.** 1998. Experimental *Helicobacter pylori* infection induces antral gastritis and gastric mucosa-associated lymphoid tissue in guinea pigs. Infect. Immun. **66:**2614–2618.
23. **Steere, A. C., P. H. Duray, and E. C. Butcher.** 1988. Spirochetal antigens and lymphoid cell surface markers in Lyme synovitis. Comparison with rheumatoid synovium and tonsillar lymphoid tissue. Arthritis Rheum. **31:**487–495.
24. **Wang, G., P. G. Boulton, N. W. Chan, M. M. Palcic, and D. E. Taylor.** 1999. Novel Helicobacter pylori alpha1,2-fucosyltransferase, a key enzyme in the synthesis of Lewis antigens. Microbiology **145**(Pt 11)**:**3245–3253.
25. **Ward, J. M., J. G. Fox, M. R. Anver, D. C. Haines, C. V. George, M. J. Collins, Jr., P. L. Gorelick, K. Nagashima, M. A. Gonda, R. V. Gilden, et al.** 1994. Chronic active hepatitis and associated liver tumors in mice caused by a persistent bacterial infection with a novel Helicobacter species. J. Natl. Cancer Inst. **86:**1222–1227.
26. **Yasoshima, M., Y. Nakanuma, K. Tsuneyama, J. Van de Water, and M. E. Gershwin.** 1995. Immunohistochemical analysis of adhesion molecules in the microenvironment of portal tracts in relation to aberrant expression of PDC-E2 and HLA-DR on the bile ducts in primary biliary cirrhosis. J. Pathol. **175:**319–325.
27. **Yoneyama, H., K. Matsuno, Y. Zhang, M. Murai, M. Itakura, S. Ishikawa, G. Hasegawa, M. Naito, H. Asakura, and K. Matsushima.** 2001. Regulation by chemokines of circulating dendritic cell precursors, and the formation of portal tract-associated lymphoid tissue, in a granulomatous liver disease. J. Exp. Med. **193:**35–49.

Editor: B. B. Finlay